

SCIENTIFIC REPORTS

OPEN

Quantitative HDL Proteomics Identifies Peroxiredoxin-6 as a Biomarker of Human Abdominal Aortic Aneurysm

Received: 08 August 2016
Accepted: 09 November 2016
Published: 09 December 2016

Elena Burillo^{1,*}, Inmaculada Jorge^{2,*}, Diego Martínez-López¹, Emilio Camafeita², Luis Miguel Blanco-Colio¹, Marco Trevisan-Herraz², Iakes Ezkurdia², Jesús Egidio³, Jean-Baptiste Michel⁴, Olivier Meilhac⁵, Jesús Vázquez^{2,*} & Jose Luis Martin-Ventura^{1,*}

High-density lipoproteins (HDLs) are complex protein and lipid assemblies whose composition is known to change in diverse pathological situations. Analysis of the HDL proteome can thus provide insight into the main mechanisms underlying abdominal aortic aneurysm (AAA) and potentially detect novel systemic biomarkers. We performed a multiplexed quantitative proteomics analysis of HDLs isolated from plasma of AAA patients (N = 14) and control study participants (N = 7). Validation was performed by western-blot (HDL), immunohistochemistry (tissue), and ELISA (plasma). HDL from AAA patients showed elevated expression of peroxiredoxin-6 (PRDX6), HLA class I histocompatibility antigen (HLA-I), retinol-binding protein 4, and paraoxonase/arylesterase 1 (PON1), whereas α -2 macroglobulin and C4b-binding protein were decreased. The main pathways associated with HDL alterations in AAA were oxidative stress and immune-inflammatory responses. In AAA tissue, PRDX6 colocalized with neutrophils, vascular smooth muscle cells, and lipid oxidation. Moreover, plasma PRDX6 was higher in AAA (N = 47) than in controls (N = 27), reflecting increased systemic oxidative stress. Finally, a positive correlation was recorded between PRDX6 and AAA diameter. The analysis of the HDL proteome demonstrates that redox imbalance is a major mechanism in AAA, identifying the antioxidant PRDX6 as a novel systemic biomarker of AAA.

Abdominal aortic aneurysm (AAA) is a major health problem, with a prevalence of ~2% in adults aged over 65 years^{1,2} and causing about 1–2% of male deaths in economically developed societies³. Clinically, AAA is defined as a permanent dilation of the aortic diameter by more than 3 cm or more than 50% of the initial value. Mechanistically, AAA is characterized by the formation of an intraluminal thrombus (ILT), proteolysis, oxidative stress, immune inflammatory response, angiogenesis and fibrosis. Currently, the only way to prevent aortic rupture in patients with an AAA >5.5 cm is surgery. AAA is usually asymptomatic and is often detected as an incidental finding during the investigation of an unrelated problem or as a consequence of radiological screening. Moreover, diameter growth is discontinuous, with periods of growth alternating with periods of stability, making prognosis difficult⁴. There is thus a pressing need to identify novel biomarkers of the presence and evolution of AAA, which provide insight into the pathological mechanisms of the disease.

The most convenient source of a systemic AAA biomarker is blood plasma. Our group and others have previously analyzed AAA patient plasma using a variety of proteomics approaches^{5–9}. However, the high dynamic range of protein concentrations in plasma makes it difficult to quantify proteins present in low amounts, even after depletion of the most abundant proteins. To circumvent this problem, some authors have concentrated on the analysis of specific plasma subproteomes, such as high-density lipoproteins (HDLs).

¹Vascular Research Lab, IIS-Fundación Jiménez Díaz-Autonomous University, Madrid, Spain. ²Cardiovascular Proteomics Laboratory, Centro Nacional de Investigaciones Cardiovasculares (CNIC), Madrid, Spain. ³Centro de Investigación Biomédica en Red de Diabetes y Enfermedades Metabólicas Asociadas (CIBERDEM), Spain. ⁴Inserm, U698, Université Paris 7, CHU X-Bichat, Paris, France. ⁵Diabète athéromatose Thérapies Réunion Océan Indien (UMR DÉTROU U1188) – Université de La Réunion-CYROI- 2, rue Maxime Rivière 97490 Sainte Clotilde – La Réunion – France. *These authors contributed equally to this work. Correspondence and requests for materials should be addressed to J.V. (email: jvazquez@cnic.es) or J.L.M.-V. (email: jlmartin@fjd.es)

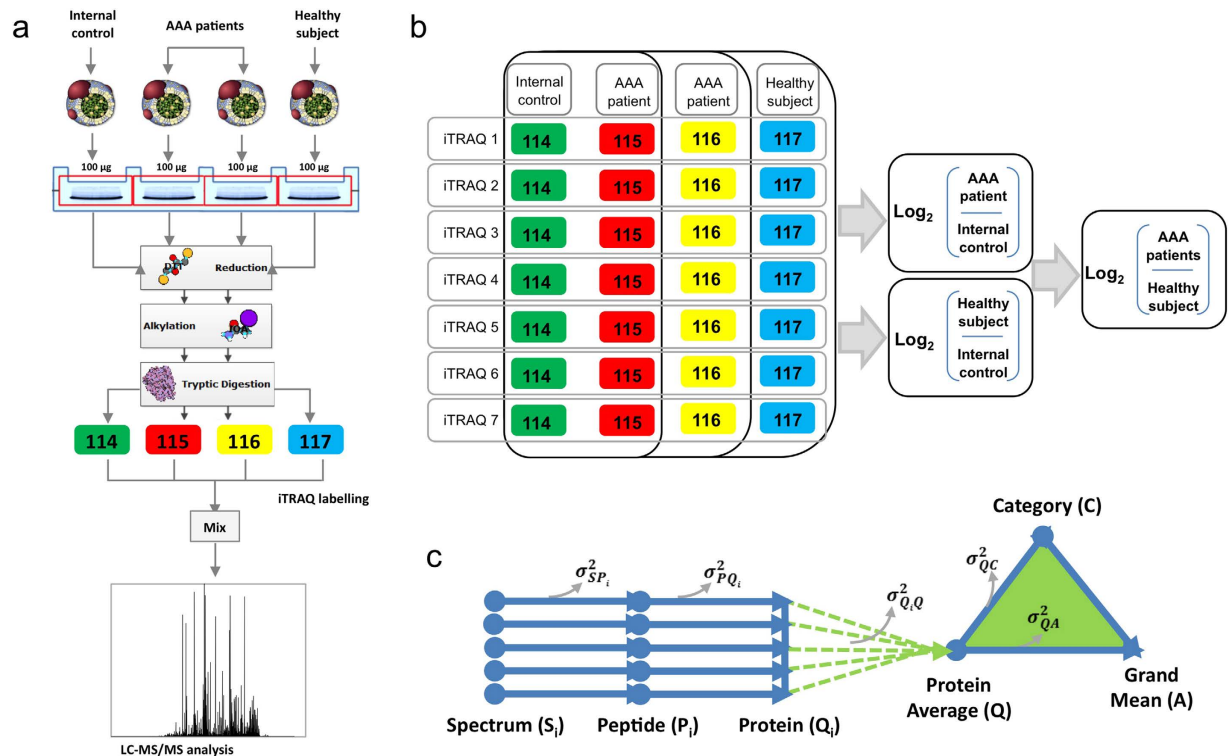


Figure 1. Multiplexed analysis of individual HDL proteomes from AAA patients: shotgun proteomics workflow. (a) HDL particles were isolated by sequential ultracentrifugation. Protein extracts were loaded onto SDS-PAGE gels, and proteins were concentrated in the stacking gel. After in-gel trypsin digestion, peptides were labeled with 4-plex iTRAQ reagents and then analyzed by LC-MS/MS. (b) A total of 7 iTRAQ experiments were performed. In each experiment, samples from 2 AAA patients and 1 control subject were compared with an internal control. The internal control was a pool of all the individual samples used in the study. (c) The statistical model for the quantitative data decomposes the total technical variance into the spectral, peptide, and protein variance components and provides a general framework to fully integrate quantitative and error information, allowing a comparative analysis of the results obtained from the 7 iTRAQ experiments.

HDLs are a transport platform of lipids and proteins. HDLs are responsible for transporting excess cholesterol from peripheral tissues to the liver for its elimination in feces and bile. Clinical and epidemiological studies consistently link low HDL cholesterol levels to an elevated risk of cardiovascular disease. A recent meta-analysis also revealed a negative association of HDL cholesterol levels with AAA in most studies¹⁰. HDLs are additionally a transport platform for constitutive and non-permanently associated plasma proteins. Screening of the HDL proteome has identified dramatic protein alterations in a variety of disease contexts, including cardiovascular diseases^{11–15}. HDLs have several important cardiovascular protective properties, including anti-oxidant, anti-inflammatory, and antithrombotic effects^{16,17}. These properties are attributable to HDL-associated proteins, and it is increasingly accepted that HDL composition, rather than quantity, is more important for its vasculo-protective activities. We previously demonstrated impaired anti-proteolytic¹⁸ and anti-oxidative functions¹⁹ in HDLs from human AAA. This effect has been linked to altered HDL protein composition or to impaired function of individual components. However, the protein alterations taking place in the HDL proteome in AAA have not been reported to date.

Here, we performed a multiplexed quantitative proteomics study of HDL-protein alterations in AAA. Systems biology analysis revealed an association of AAA with an increased HDL content of proteins related to redox homeostasis, most clearly evident in the increased levels of peroxiredoxin-6 (PRDX6). Circulating levels of PRDX6 are also increased in AAA-patient plasma, and PRDX6 levels correlate positively with AAA size, identifying PRDX6 as a promising biomarker of AAA.

Results

Analysis of the human HDL proteome in AAA. HDL particles were isolated from plasma and subjected to trypsin digestion. The resulting peptides were iTRAQ-labeled and combined in 7 independent experiments for LC-MS/MS analysis (Fig. 1). The protein composition of the HDL samples was characterized by spectral counting of the 7 HDL pools. At a 1% FDR threshold, 112 proteins were identified as HDL particle constituents in at least 3 experiments (Supplementary Table S1). As expected, ApoA1 was one of the most abundant HDL proteins, representing 33% of total protein composition. Other abundant HDL proteins were α -1-antitrypsin, complement C3, apolipoproteins D, E and M, and paraoxonase/arylesterase 1 (3–4% each) (Supplementary Figure S1). Albumin and ApoB100 were also identified but were not included in the analysis because they are abundant

Gene name	Accession number	Protein name	Xq = Log ₂ (AAA/control)														Integration data				
			Individual comparatives														Xq	p-value	FDR		
			1	2	3	4	5	6	7	8	9	10	11	12	13	14					
Redox/homeostasis-related proteins	PRDX6	P30041	PRDX6_HUMAN Peroxisidin-6	1.12	0.77	1.78	1.59	1.62	0.58	1.29	3.78	0.0002	0.0116								
	RRF4	P02753	RET4_HUMAN Retinol-binding protein 4	1.71	2.32	1.02	1.45	1.43	1.89	2.26	0.35	0.71	0.75	0.69	0.82	0.77	0.23	1.08	0.0003	0.0176	
	PON1	P27169	PON1_HUMAN Serum paraoxonase/arylesterase 1	0.16	1.24	1.88	0.95	1.02	1.22	1.55	0.57	0.47	0.03	1.74	1.58	-0.05	1.01	0.95	1.34	0.0008	0.0309
	CST3	P01034	CYTC_HUMAN Cystatin-C	0.42	1.56	1.09	1.19	1.38	2.42	2.66	0.69	0.66	1.01	0.54	1.11	1.69	1.37	0.87	2.58	0.0029	0.0847
	APOA4	P06727	APOA4_HUMAN Apolipoprotein A-IV	0.50	1.11	0.73	0.59	1.00	0.74	0.21	-0.13	-0.19	0.18	-0.25	-0.04	-0.13	-0.60	0.26	1.04	0.2976	0.9804
	HBA1	P69905	HBA_HUMAN Hemoglobin subunit alpha	-0.41	-0.45	0.54	-0.02	0.29	0.37	0.25	0.62	0.02	0.05	0.09	0.20	2.55	-0.06	0.26	1.00	0.3196	0.9967
	HBB	P68871	HBB_HUMAN Hemoglobin subunit beta	-0.02	0.08	2.12	0.12	0.18	-0.25	0.00	1.00	-0.03	0.01	0.53	-0.49	3.29	0.93	0.11	0.50	0.6155	1.0074
	PON3	Q15166	PON3_HUMAN Serum paraoxonase/lactonase 3	0.04	0.33	1.18	0.07	-0.54	-0.25	-0.15	0.23	0.42	0.61	-0.09	-0.01	0.27	-0.06	0.05	0.33	0.7432	1.0017
	HP	P00738	HPT_HUMAN Haptoglobin	-0.47	1.65	0.31	1.04	2.35	0.86	-0.15	-0.84	-1.18	0.67	0.89	0.47	1.58	1.26	0.03	0.05	0.9629	1.0009
	HLA-A*23	P30447	LA23_HUMAN HLA class I histocompatibility antigen, A-23 alpha chain	1.19	0.53	1.26	1.83	1.65	1.34	0.61	2.74	1.13	3.59	0.0004	0.0211						
B2M	P51769	B2MG_HUMAN Beta-2-microglobulin	0.41	1.55	0.63	0.29	0.65	0.36	0.16	0.24	0.63	1.04	0.06	0.46	1.77	0.01	2.12	0.0339	0.4253		
HLA-A*1	P30443	LA01_HUMAN HLA class I histocompatibility antigen, A-1 alpha chain	2.79	0.33	0.06	1.21	1.04	1.20	0.02	-0.88	0.08	1.64	0.39	2.97	1.82	0.13	0.33	1.21	0.2263	0.9391	
UBA52	P62937	RLA0_HUMAN Ubiquitin-SOS-ribosomal protein L40	0.37	0.20	0.16	-0.21	1.35	0.92	0.32	0.26	0.04	0.30	-0.47	0.03	0.33	1.18	0.2381	0.9578			
AZP1	P25311	ZAG2_HUMAN Zinc-alpha-2-glycoprotein	0.93	0.67	0.84	0.75	0.22	0.03	0.03	-0.44	1.59	0.39	-0.70	0.16	0.62	0.5376	0.9670				
SAA	E9PQD6	E9PQD6_HUMAN Serum amyloid A protein	-0.31	1.82	-0.65	1.52	0.00	-0.28	0.00	0.00	0.00	0.00	0.00	0.00	0.00	0.94	2.78	0.0055	0.1454		
LBP	P18428	LBP_HUMAN Lipopolysaccharide-binding protein	0.36	0.14	0.68	1.25	1.46	0.57	0.36	0.17	0.72	-0.11	0.42	1.46	0.28	0.32	0.55	1.94	0.0530	0.5582	
SAA	P0D1J8	SAA1_HUMAN Serum amyloid A-1 protein	1.86	1.60	-1.07	0.23	-0.22	-0.71	-0.44	0.45	0.33	-0.58	0.17	0.40	2.24	-0.11	0.44	1.59	0.1124	0.8227	
AHSG	P02765	FETUA_HUMAN Alpha-2-HS-glycoprotein	0.51	0.95	1.15	0.85	1.20	-0.25	0.37	-0.47	-0.06	-0.17	-0.07	-0.05	0.07	-0.04	0.35	1.33	0.1838	0.9139	
SAA	D3DQX7	D3DQX7_HUMAN Serum amyloid A protein	0.36	-0.86	-0.24	0.08	-0.23	0.66	1.15	-0.23	0.63	0.70	-0.31	0.47	0.29	1.05	0.2946	0.9826			
SAA2	P0D1J9	SAA2_HUMAN Serum amyloid A-2 protein	1.44	0.55	-1.10	0.64	-1.10	0.34	-0.02	-0.59	0.14	0.86	0.26	0.95	0.3408	1.0146					
ITIH4	Q14624	ITIH4_HUMAN Inter-alpha-trypsin inhibitor heavy chain H4	-1.14	-0.71	-0.27	2.08	1.07	2.52	-0.38	0.63	-1.53	-1.19	-0.65	-2.35	0.12	0.52	0.6012	1.0122			
ORM1	P02763	A1AG1_HUMAN Alpha-1-acid glycoprotein 1	-0.71	0.42	-0.52	1.42	1.14	1.69	0.89	-0.35	-0.07	-0.22	1.77	0.44	-0.67	-0.09	0.12	0.52	0.6015	1.0095	
ORM2	P19652	A1AG2_HUMAN Alpha-1-acid glycoprotein 2	-0.49	-0.15	0.03	0.35	0.73	1.63	1.42	-0.22	-0.31	-0.22	0.32	-0.07	-0.32	-0.38	0.09	0.42	0.6745	1.0098	
SAA	B2R5G8	B2R5G8_HUMAN Serum amyloid A protein	0.71	0.79	-0.21	-0.20	-0.82	-0.59	-0.67	0.62	-0.21	0.11	0.13	-0.46	1.06	0.01	0.03	0.24	0.8128	1.0056	
SAA4	P35542	SAA4_HUMAN Serum amyloid A-4 protein	0.42	-0.48	-0.21	-0.32	-0.68	-0.54	-0.06	0.42	0.898	0.24	0.09	-0.07	1.31	0.03	0.00	0.15	0.8771	1.0137	
HP	P00738	HPT_HUMAN Haptoglobin	-0.47	1.65	0.31	1.04	2.35	0.86	-0.15	-0.84	-1.18	0.67	0.89	0.47	1.58	1.26	0.03	0.05	0.9629	1.0009	
SERPINA1	P01009	A1AT_HUMAN Alpha-1-antitrypsin	-0.09	0.74	0.37	0.06	0.97	0.22	-1.51	-0.44	-0.22	-1.21	-0.38	-2.29	-0.09	-0.16	0.8717	1.0141			
SERPINF2	P08697	A2AP_HUMAN Alpha-2-antiplasmin	-0.04	-0.08	-0.55	-1.10	-0.04	-0.13	-0.65	-0.26	0.62	0.5338	0.9701								
PFN1	P07737	PROF1_HUMAN Profilin-1	1.16	0.11	1.30	2.04	1.24	-0.39	1.10	1.57	0.48	1.12	0.14	1.10	0.90	3.04	0.0024	0.0730			
PF4	P02776	PLF4_HUMAN Platelet factor 4	0.06	0.65	0.51	1.84	0.00	0.00	0.23	0.40	0.79	2.55	0.108	0.2370							
PBBP	P02775	CXCL7_HUMAN Platelet basic protein	0.60	0.43	0.12	0.44	0.84	1.44	-0.07	1.55	0.04	1.20	0.38	-0.19	1.14	0.37	0.60	2.13	0.031	0.4364	
RAP1A	P62834	RAP1A_HUMAN Ras-related protein Rap-1A	-0.09	0.00	2.10	1.24	0.52	0.86	3.31	1.52	1.00	1.10	0.65	1.98	0.479	0.5151					
PLA2G7	Q13093	PAFA_HUMAN Platelet-activating factor acetylhydrolase	1.63	0.95	0.97	-0.47	-0.86	-0.08	-0.62	0.23	0.37	0.74	0.47	0.48	1.24	1.07	0.43	1.54	0.1244	0.8192	
PF4V1	P10720	PF4V_HUMAN Platelet factor 4 variant	-0.25	0.35	-0.09	0.10	0.38	1.67	0.47	0.33	0.60	0.18	0.46	-0.07	0.27	1.49	0.1411	0.8171			
ACTA2	P62736	ACTA_HUMAN Actin, aortic smooth muscle	0.31	0.16	-0.06	1.10	1.10	2.23	-1.03	1.25	1.31	1.87	0.82	1.47	2.28	0.93	0.77	2.67	0.0072	0.1724	
CNDP1	Q96RN2	CNDP1_HUMAN Beta-His-His dipeptidase	1.41	0.99	1.85	1.31	1.41	1.27	1.62	0.16	0.54	-0.36	0.62	-0.02	-0.53	0.48	0.72	2.52	0.0117	0.2474	
LPA	Q11HF67	Q11HF67_HUMAN Lipoprotein, Lp(a)	2.26	2.39	1.14	1.10	0.60	1.16	0.10	0.17	0.79	2.46	0.0448	0.3893							
SERPINF1	P36955	PEDF_HUMAN Pigment epithelium-derived factor	0.83	1.32	0.66	1.59	1.92	1.78	1.34	-0.30	0.18	0.04	0.01	0.45	-0.60	-0.16	0.64	2.28	0.0226	0.3507	
GC	P02774	VTDB_HUMAN Vitamin D-binding protein	0.58	1.08	0.61	1.15	2.17	1.52	1.96	-0.16	-0.21	0.11	-0.15	0.34	0.00	-0.10	0.64	2.27	0.0235	0.3539	
LOC613037	A8MR75	K220L_HUMAN Putative NPIP-like protein LOC100132247	1.50	0.73	0.66	0.15	1.47	0.44	0.92	1.78	0.69	2.18	0.0294	0.4082							
LCAT	P04180	LCAT_HUMAN Phosphatidylcholine-sterol acyltransferase	0.51	1.05	0.56	0.73	1.15	1.58	2.23	0.13	0.46	0.02	0.46	0.96	0.45	0.56	0.58	2.08	0.0372	0.4458	
AMBP	P02760	AMBP_HUMAN Protein AMBP	0.89	1.37	0.87	0.47	1.34	1.31	1.23	-0.14	0.12	0.58	-0.25	0.31	0.41	-0.36	0.57	2.04	0.0411	0.4608	
N/A	B3KNA1	B3KNA1_HUMAN cDNA FLJ14021 fis, clone HEMBA1002513, highly similar to HDAC6	0.16	-0.25	0.24	0.61	-0.28	-0.55	0.62	1.87	0.611	0.5853									
ACTB	P60709	ACTB_HUMAN Actin, cytoplasmic 1	-0.08	0.24	-0.17	0.88	0.53	0.43	-0.67	0.88	0.79	1.22	0.69	0.62	0.85	0.75	0.47	1.68	0.0928	0.7193	
PGBD3	Q8N328	PGBD3_HUMAN P1ggyBac transposable element-derived protein 3	0.66	1.22	1.22	0.27	0.02	0.10	0.59	1.78	0.0755	0.6522									
DSG1	Q02413	DSG1_HUMAN Desmoglein-1	1.42	-0.01	0.32	-1.11	0.22	-0.29	0.05	-0.64	-0.54	-1.53	0.1259	0.8193							
APOH	P02749	APOH_HUMAN Beta-2-glycoprotein 1	-0.44	-0.72	0.06	-0.53	-0.78	-0.84	-0.38	0.09	0.00	1.29	-0.43	-0.71	-0.69	-1.26	-0.56	-1.75	0.0805	0.6632	
IGLL5	B9A064	IGLL5_HUMAN Immunoglobulin lambda-like polypeptide 5	-0.12	3.42	-0.24	-0.61	-1.10	-1.49	-0.61	-0.34	0.25	-0.98	-1.04	-0.45	-0.62	-1.90	0.0572	0.5685			
MMRN2	Q9H8L6	MMRN2_HUMAN Multimerin-2 OS	-1.15	-1.05	-0.81	-0.54	-1.15	-0.34	-0.72	1.91	0.0562	0.5698									
C2orf15	Q8WU43	CB015_HUMAN Uncharacterized protein C2orf15	-0.01	1.90	2.74	0.02	-0.17	0.71	-0.85	-0.28	0.0259	0.3696									
IGHM	P01871	IGHM_HUMAN Ig mu chain C region	-0.18	-0.62	-0.49	-0.13	2.10	0.20	1.66	-0.38	1.18	-0.04	-0.23	2.92	0.06	-1.02	-0.71	-0.31	0.0256	0.3752	
TF	P02787	TRFE_HUMAN Tumor necrosis factor	-0.32	2.04	-0.07	-1.04	2.10	1.84	-0.45	-1.08	-0.36	-0.99	-0.64	-0.50	-0.84	-0.40	-0.0079	0.1800			
A2M	P01023	A2MG_HUMAN Alpha-2-macroglobulin	0.38	0.93	0.29	1.48	1.18	0.26	0.74	1.38	1.49	0.47	0.0008								
C9	P02748	C9_HUMAN Complement component C9	0.66	-0.09	0.66	0.69	0.67	-0.16	-0.32	0.34	0.24	0.00	0.42	0.33	0.45	0.20	0.84	0.4024	1.0195		
CO4A	P0C0L4	CO4A_HUMAN Complement C4-A	-0.85	-0.02	0.41	0.32	1.18	1.67	0.58	0.16	0.12	0.06	-0.13	-0.11	-0.19	-0.58	0.03	0.25	0.8046	1.0072	
SERPINC1	P05155	IC1_HUMAN Plasma protease C1 inhibitor	0.35	-0.91	-1.30	-0.36	-1.15	1.25	-0.42	1.15	0.40	-0.51	-0.86	-0.51	-0.06	-1.06	-0.29	0.84	0.3983	1.0140	
CLU	P10909	CLUS_HUMAN Clusterin	-0.22	-0.39	0.00	-0.17	-0.27	-0.56	0.30	-0.04	-0.08	-0.36	0.44	-0.36	-0.33	-0.56	0.30	-0.90	0.3666	1.0223	
IGKC	P01834	IGKC_HUMAN Ig kappa chain C region	0.06	-0.82	0.15	-0.38	-0.40	-0.94	-0.66	-0.19	-0.57	0.59	-0.31	-0.45	-0.06	-0.35	-0.31	-0.52	0.3566	1.0186	
IGHG2	P01859	IGHG2_HUMAN Ig gamma-2 chain C region	-0.18	-0.59	-0.56	-1.23	-1.67	-1.31	-0.50	-0.13	0.39	1.02	0.36	-0.04	-0.52	-1.93	0.1263	0.8018			
IGHG1	P01857	IGHG1_HUMAN Ig gamma-1 chain C region	-0																		

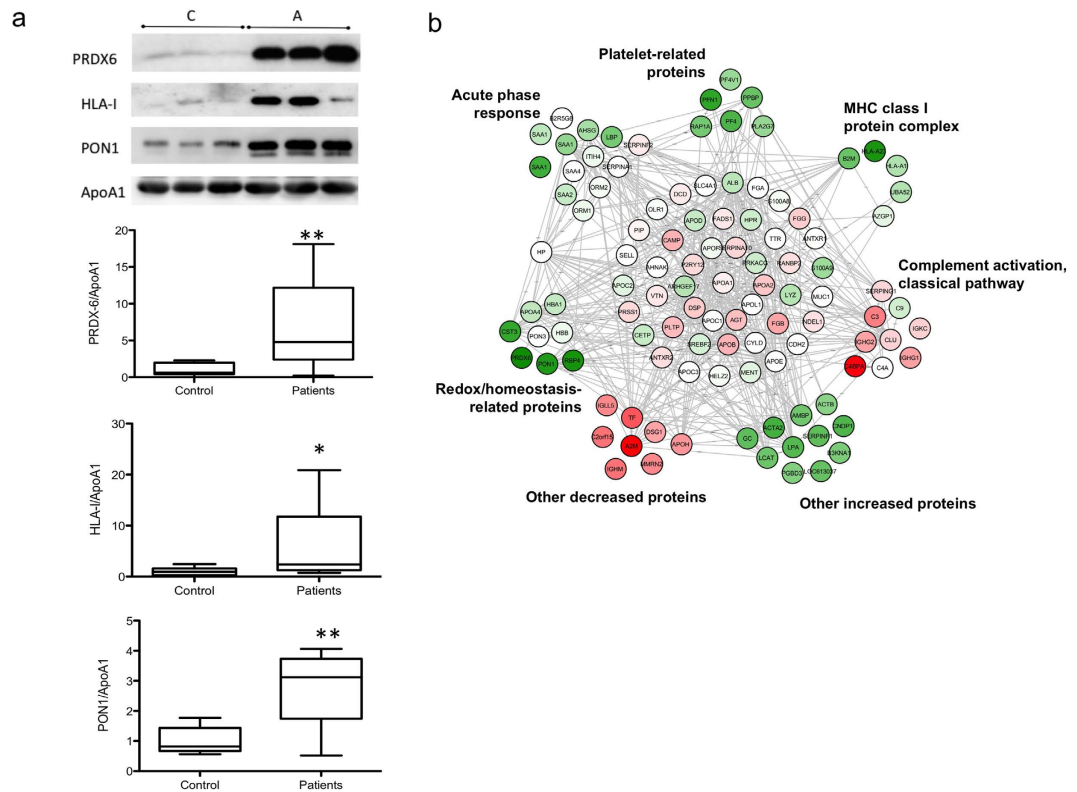


Figure 3. Validation and interaction network of the AAA HDL proteome. (a) Representative protein validation by western blot. The quantitative results for PRDX6, HLA-I, and PON1 correspond to the same 14 AAA and 7 control samples used in the proteomic analysis. * $p < 0.05$, ** $p < 0.01$. (b) Interaction network of HDL proteins showing the quantitative data. Significant category changes were clustered.

network analysis, which indicated that most of the altered HDL proteins were interconnected in a dense interaction network containing most of the quantified HDL proteins (Fig. 3b).

Tissue expression of PRDX6 in AAA. Of the validated proteins, we focused on PRDX6 because it reflects the generalized alteration in proteins implicated in redox homeostasis, the functional category most clearly changed in the HDL proteome of AAA patients. Immunohistochemical analysis of PRDX6 expression and localization in the ILT obtained from AAA patients revealed intense PRDX6 immunostaining associated with areas of neutrophil infiltration and RBC degeneration (Figs 4 and 5). Examination of the aortic wall of AAA patients showed strong PRDX6 staining in cholesterol-rich and acellular atherosclerotic plaques in the media layer, but also revealed PRDX6 colocalization with vascular smooth muscle cells (VSMCs) (Fig. 4). PRDX6 also colocalized in AAA tissue with the lipid peroxidation marker MDA and with ceroids, markers of RBC-associated oxidation (Fig. 5).

Circulating PRDX6 in AAA patients. The association of PRDX6 with circulating HDL particles could arise from interaction of HDL particles with circulating cells or from direct loading from plasma. The localization of PRDX6 in areas of erythrophagocytosis suggested that the presence of PRDX6 in HDL particles could arise, at least in part, from the interaction of HDLs with circulating RBCs. To test this hypothesis, we incubated HDLs isolated from healthy subjects with intact or lysed RBCs, and then re-isolated the HDLs to analyse PRDX6 content. PRDX6 levels were low in untreated HDLs from healthy subjects, but increased markedly when incubated with intact or lysed RBCs (Fig. 6). In control experiments, the abundant RBC protein catalase was taken up by HDL particles incubated with lysed RBCs but not by particles incubated with intact RBCs.

Given that HDL is a platform of plasma-associated proteins, we also examined whether PRDX6 is present in plasma and could serve as a circulating biomarker of AAA. The plasma concentration of PRDX6 was analyzed in a cohort of control individuals ($N = 27$) and AAA patients ($N = 47$). Cohort clinical characteristics are shown in Table 1. This analysis confirmed the presence of PRDX6 in plasma, which to our knowledge has not been reported before, and also revealed higher plasma PRDX6 levels in AAA patients than in controls (21 ± 2 vs 10 ± 2 ng/mL; $p < 0.01$) (Fig. 7a). Multivariate logistic regression analysis of AAA risk factors revealed plasma PRDX6 concentration, hypertension, and smoking to be independent predictors of the presence of AAA [Odds Ratio CI (95%): 1.060 (1.006–1.117), $p < 0.05$ for PRDX6; 5.775 (1.670–19.973), $p < 0.01$ for hypertension; and 10.028 (1.139–88.311), $p < 0.05$ for smoking]. Furthermore, plasma PRDX6 level correlated positively with AAA size ($r = 0.4$, $p < 0.001$, adjusted for age) (Fig. 7b), reinforcing the potential of PRDX6 as a biomarker of AAA.

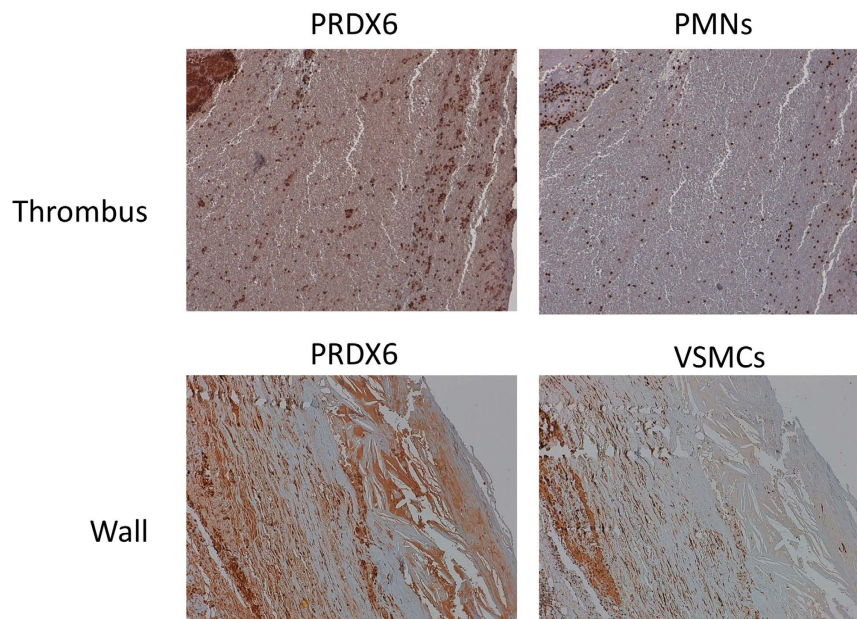


Figure 4. PRDX6 immunohistochemistry in AAA tissue. PRDX6 was detected in AAA thrombus (colocalizing with neutrophils: PMNs, CD15 staining) and wall (colocalizing with vascular smooth muscle cells: VSMC, alpha actin staining). Magnification x10. N = 10.

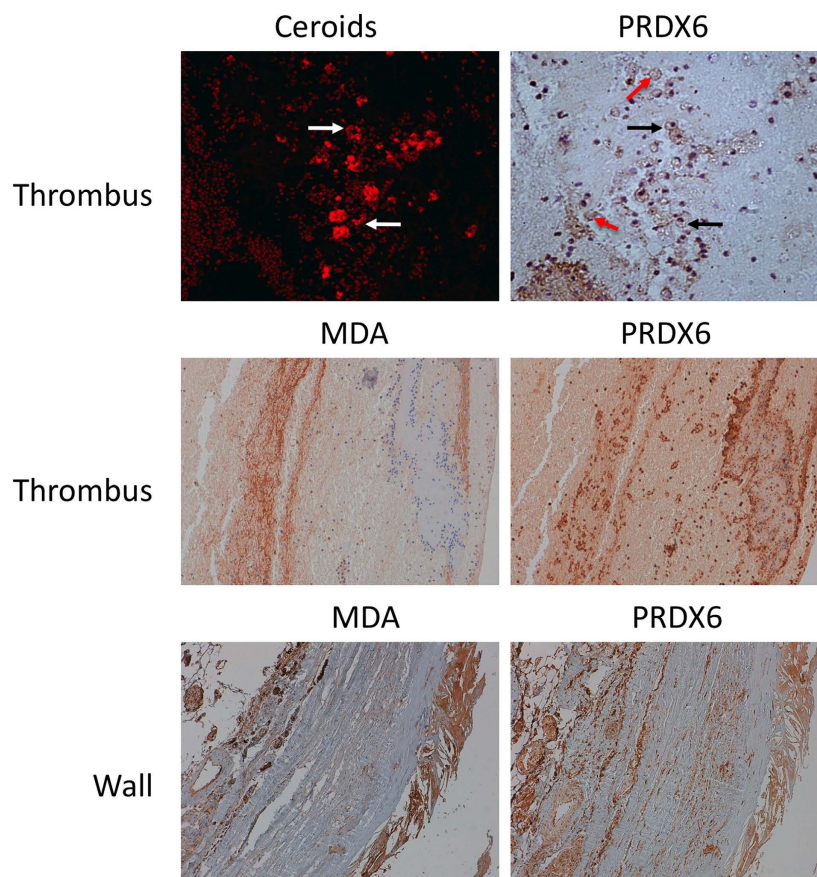


Figure 5. PRDX6 is expressed in areas of high oxidative stress in AAA tissue. PRDX6 colocalizes with ceroids and the lipid peroxidation marker MDA in AAA thrombus and wall. Black arrow indicates typical ceroid rings; red arrow indicates degenerated red blood cells. Magnification x10 (x40 in the upper part of ceroids and PRDX6). N = 10.

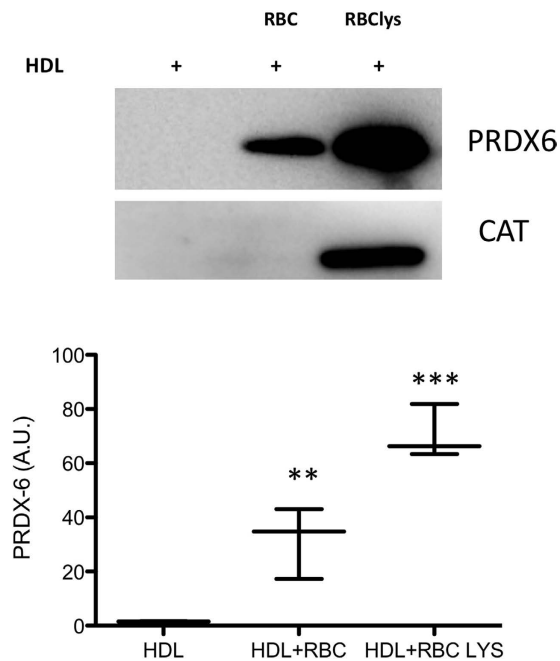


Figure 6. PRDX6 protein levels in HDL after incubation with RBCs. Western blot of PRDX6 and catalase (CAT) in HDL samples incubated with red blood cells (RBC) and lysed RBCs (RBClys). Quantification of densitometric analysis is shown (N = 3). **p < 0.01, ***p < 0.001.

iTRAQ HDL	Control (N = 7)	AAA (N = 14)	p-Value
Sex (male/female)	7/0	14/0	ns
Age (years ±SD)	64.9 ± 0.2	66.5 ± 1.2	0.024
Dyslipidemia (%)	64.9	64.9	ns
Current smoker (%)	71.4	50	ns
Diabetes (%)	14.3	14.3	ns
Hypertension (%)	42.9	64.3	ns
Heart Disease (%)	28.6	35.7	ns
Statins (%)	42.9	85.7	0.006
ELISA PRDX6	Control (N = 27)	AAA (N = 47)	p-Value
Sex (male/female)	27/0	47/0	ns
Age (years ±SD)	64.9 ± 0.2	66.1 ± 5.5	ns
Dyslipidaemia (%)	55.6	56.5	ns
Current smoker (%)	7.4	38.3	0.03
Diabetes (%)	7.4	19.1	ns
Hypertension (%)	25.9	63.8	0.01
Heart Disease (%)	18.5	17	ns
Statins (%)	11.1	38.3	ns

Table 1. Clinical characteristics of patients and control participants.

Discussion

HDLs are a complex and heterogeneous family of particles with different lipid and protein cargo and functionality. Different methodologies can be used to isolate HDLs, and not all HDL subpopulations are equivalent. In this study, we isolated HDLs by the well-established ultracentrifugation method to isolate most particle subclasses and obtain a general proteomics view of HDLs²¹. However, it is important to note that the small size of HDLs means that all the proteins detected and quantified by mass spectrometry are unlikely to reside in the same particle simultaneously. HDLs are currently regarded as a transport platform of constitutive and non-permanently associated lipids and proteins that may have specific functions in disease¹⁷. Our analysis identified and quantified 112 proteins that are consistently associated with HDLs in AAA, of which 34 proteins (8% of HDL by composition) have not been previously characterized as HDL components. Quantitative proteomics demonstrated that HDLs in AAA patients are particularly enriched in PRDX6, HLA-I, retinol-binding protein 4, and PON1 and are depleted in C4b-binding protein alpha chain and α -2 macroglobulin, among others. Systems biology analysis

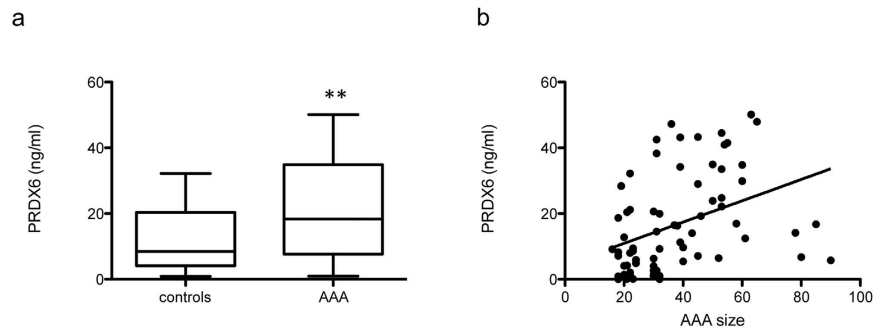


Figure 7. ELISA analysis of PRDX6 in AAA patient plasma. (a) Plasma concentration of PRDX6 in a cohort of control participants (N = 27) and AAA patients (N = 47) (** $p < 0.01$). (b) Correlation between PRDX6 and AAA size ($r = 0.4$, $p < 0.001$, age-adjusted).

demonstrated that these prominent changes reflect a general increase in proteins related to redox homeostasis, acute-phase response, and platelet activation and a decrease in proteins related to complement activation.

The levels and functionality of HDLs are altered in immune inflammatory diseases such as rheumatoid arthritis and systemic lupus erythematosus (SLE)²². Interestingly, serum amyloid A, one of the HDL components we found to be increased in AAA, has been suggested to underlie the impaired anti-inflammatory properties of HDL in SLE patients²³, and lack of endogenous acute-phase serum amyloid A protects against experimental AAA²⁴. We also found that AAA patients have below-normal levels of C3, consistent with our previous finding that C3 declines in AAA patient plasma, contrasting its accumulation, consumption, and activation in the AAA thrombus²⁵. In addition to the known role of HDLs in the humoral response through modulation of the complement system, HDL particles may also influence the innate and adaptive immune responses by modulating antigen presentation functions in macrophages, B cells, and T cells²⁶. In line with this idea, we found that HDLs from AAA patients have increased levels of HLA-I, a central immune system molecule that presents endoplasmic-reticulum-derived peptides. The identification of HLA-I in HDL supports the role of HDL as a platform for the assembly of innate immune complexes²⁷. Wang *et al.* demonstrated that dysfunctional HDLs promote lipid raft disruption, resulting in less control of antigen presentation and T cell activation²⁸. Together, these results support an important role for HDLs in innate and adaptive immune responses, not only as a passive transport platform, but also through the active contribution of constituent proteins.

Proteins with roles in redox balance have been previously observed in HDLs¹². Here, PON1 and PRDX6, two proteins implicated in oxidative stress, were increased in HDL from AAA patients. PON1 is known for its HDL-associated antioxidant capacity²⁹. Vaisar *et al.*¹² reported elevated HDL PON1 content in patients with coronary artery disease, fitting well with our observation in AAA patients. However, we recently found that serum PON1 activity is decreased in AAA patients³⁰, suggesting that PON1 activity is impaired in HDLs of AAA patients. PRDX6 belongs to the peroxiredoxin family, a set of enzymes implicated in the protection against oxidation and the control of H₂O₂ signaling³¹. Other members of the PRDX family have been previously associated with AAA, such as PRDX-1 and PRDX-2^{32,33}. However, this is the first time that PRDX6 has been associated with both HDL and AAA. PRDX6 is a bifunctional enzyme, with glutathione peroxidase and phospholipase A2 (PLA2) activities. Because of this dual function, the precise role of PRDX6 is not yet completely understood. Similar to other PRDXs, PRDX6 is able to reduce short-chain hydroperoxides through its peroxidase activity. However, the PLA2 activity specific to PRDX6 has been linked not only to antioxidant properties³⁴ but also to pro-oxidant properties³⁵. Very recently, PRDX6 expression was shown to support higher Nox1-derived superoxide production, which was reduced by an inhibitor of PRDX6 phospholipase A2 activity³⁶. The impaired antioxidant function reported in HDLs from AAA patients¹⁹ will likely be the result of the imbalance between the levels and activities of the various pro- and antioxidant proteins, including PRDX6.

Previous studies of AAA tissue have shown increased levels of various proteins involved in redox balance. Elevated levels have been reported of the antioxidant proteins thioredoxin-1, PRDX1, and catalase in AAA thrombus, associated with both RBCs and neutrophils³⁷. In the present study, high PRDX6 levels were also observed in AAA thrombus, mainly in areas of degenerated RBCs (in the process of erythrophagocytosis) and neutrophils. It is important to note that PRDX6 relocates to the cell membrane during neutrophil activation³⁸, which is required for optimal NADPH oxidase activity. The localization of PRDX6 in VSMCs of the AAA wall is probably a response to increased oxidative stress³⁹, since PRDX6 expression in VSMCs is known to increase in response to H₂O₂⁴⁰. Other oxidative stress markers identified in AAA tissue include the lipid peroxidation marker MDA and ceroids, which mark oxidation associated with lipids and RBCs¹⁹. We detected colocalization of PRDX6 with ceroids and MDA in the AAA thrombus; moreover, an intense PRDX6 signal was detected in cholesterol-rich and acellular atherosclerotic plaques in the AAA wall, colocalizing with MDA-positive areas. Cell-associated PRDX6 thus might participate in redox imbalance in AAA tissue through protective antioxidant functions or deleterious neutrophil-dependent NADPH activation; however, in a highly oxidative environment such as AAA, PRDX6 may lose its antioxidant activities through oxidative modification by lipid hydroperoxides⁴¹. Whether PRDX6 plays a protective or deleterious role in AAA tissue deserves further investigation.

Our finding that *ex-vivo* incubation of HDLs with lysed RBCs increases HDL levels of PRDX6 and catalase suggests that part of the PRDX6 observed in AAA thrombus may arise from RBC lysis. However, increased levels

of PRDX6, but not catalase, were also observed in HDLs incubated with intact RBCs, suggesting that HDLs may interact directly with membrane-bound PRDX6 in RBCs. In any case, PRDX6 translocation to the cell membrane is important for reactive oxygen species production through NADPH oxidase 2 complex activation^{34,38}, suggesting that the elevated PRDX6 levels in circulating HDL of AAA patients reflect an increased systemic oxidative stress. Our study not only identifies PRDX6 as a HDL constituent, but also shows that PRDX6 concentration doubles in the plasma of AAA patients, probably reflecting the systemic response to increased oxidative stress in AAA. We also found a positive correlation between PRDX6 and AAA size, a marker of AAA progression and the clinical parameter used in the management of AAA patients.

Our analysis suggests that the altered protein profile of HDLs in AAA reflects disease events, including an increase in antioxidant proteins probably associated with a systemic response to the redox imbalance in AAA. The increased HDL and plasma levels of PRDX6 in AAA patients support the potential of PRDX6 as a new biomarker of AAA.

Methods

The authors declare that all methods were performed in accordance with the relevant guidelines and regulations.

Patient selection. The studies were approved by the Research and Ethics Committee of the Fundación Jiménez Díaz University Hospital Health Research Institute (IIS-FJD; Madrid, Spain), and patients and control participants gave informed consent for their inclusion in the study. Patients with an asymptomatic infrarenal AAA (aortic size >3 cm confirmed by abdominal ultrasound) were recruited during clinical examination or before surgical repair at the Vascular Surgery Service at FJD University Hospital. Controls with non-dilated infrarenal aortas (aortic size <3 cm, confirmed by abdominal ultrasound) were recruited through a screening program. For proteomic analysis, EDTA plasma samples were obtained from 14 male AAA patients and 7 male control participants. For ELISA, a second set of plasma samples (27 controls and 47 AAA patients) were obtained from the IIS-FJD biobank. Clinical characteristics of all controls and AAA patients are summarized in Table 1. For immunohistochemistry, samples of AAA thrombus tissue (n = 10) and wall tissue (n = 10) were collected from male patients (70 ± 6 years old, 70% hypertensive, 30% current smokers, 50% dyslipidemic, 10% diabetic, 20% heart disease) undergoing open surgical repair due to aortic dilation >5 cm at the IIS-FJD Vascular Surgery Service.

HDL isolation. Lipoproteins were isolated from individual EDTA plasma samples by ultracentrifugation as described in Supplementary Information. Moreover, additional HDLs were isolated from healthy volunteers for incubation with red blood cells (RBC)(N = 3). Briefly, HDLs were incubated with RBCs (intact or lysed with H₂O/NaCl) for 4 hours at 37 °C, and HDLs were subsequently re-isolated by ultracentrifugation.

Proteomics. Proteomic analysis was performed on HDL particles isolated from 14 AAA patients and 7 controls (Table 1). HDL samples were in-gel digested overnight at 37 °C with sequencing-grade trypsin (Promega, Madison, WI, USA) at an 8:1 protein:trypsin (w/w) ratio in 50 mM ammonium bicarbonate, pH 8.8⁴². The resulting peptides were desalted on C18 Oasis cartridges (Waters Corporation, Milford, MA, USA) using 50% acetonitrile (ACN) (v/v) in 0.1% trifluoroacetic acid (v/v) as eluent, and vacuum dried. A total of 7 independent isobaric tags were performed for relative and absolute quantitation (iTRAQ) 4-plex experiments. iTRAQ labeling was performed essentially according to the manufacturer's instructions, as previously described in detail^{42–44} (Supplementary Information). In each experiment, samples from 2 AAA patients and 1 control participant were compared with an internal control, prepared by pooling protein extracts from all subjects of the study. All the comparisons included independent biological preparations, making a total of 14 comparisons between AAA samples and the internal control sample and 7 comparisons between control samples and the internal control sample. The use of the internal control allowed comparison of data from different individuals in different experiments.

The tryptic peptide mixtures were subjected to nano-HPLC (Easy nLC 1000 liquid chromatograph, Thermo Scientific, San Jose, CA, USA) coupled to a Q Exactive mass spectrometer (Thermo Scientific). Peptides were suspended in 0.1% formic acid, loaded onto a C18 RP nano-precolumn (75 µm I.D. and 2 cm, Acclaim PepMap100, Thermo Scientific), and separated on an analytical C18 nano-column (75 µm I.D. and 50 cm, Acclaim PepMap100) in a continuous gradient increasing from 8% to 30% B over 120 min, followed by a rapid increase from 30% to 90% B over 2 min at a flow rate of 200 nL/min. The Q Exactive mass spectrometer was operated in data-dependent mode with a normal FT-resolution spectrum (70,000 resolution) in the mass range of *m/z* 390–1500, followed by acquisition of data-dependent MS/MS spectra from the 10 most intense parent ions identified in the chromatographic run.

Peptides were identified by searching against a Human Uniprot database supplemented with porcine trypsin (120501 entries; release October 2012). The search was conducted with the SEQUEST algorithm (Proteome Discoverer 1.4, Thermo Finnigan), allowing two missed cleavages and using 600 ppm precursor mass tolerance and 0.03 ppm fragment mass tolerance. Methionine oxidation and cysteine carbamidomethylation were allowed as variable modifications. For peptide iTRAQ labeling, lysine and N-terminal modifications of +144.1020 Da were selected as fixed modifications. The same MS/MS spectra collections were searched against inverted databases constructed from the same target databases. SEQUEST results were analyzed by the probability ratio method⁴⁵; false discovery rates (FDR) for peptide identification were calculated using the refined method⁴⁶. The statistical model used to analyze the quantitative data has been described before in detail⁴³ (Supplementary Information). The systems biology analysis was performed using the Systems Biology Triangle (SBT)²⁰.

The data set from the analysis of HDL proteome (raw and msf files, protein database fasta file, searching parameters xml file, and excel tables with identification and quantification data) is available in the PeptideAtlas repository (<http://www.peptideatlas.org/PASS/PASS00861>), which can be downloaded via ftp.peptideatlas.org.

Western blot. Equal amounts of HDL (20 µg) were loaded onto 10% polyacrylamide gels, electrophoresed and transferred to nitrocellulose membranes. Blots were blocked with 7% dried skimmed milk in 0.05% Tris-buffered saline and Tween (TBS-T) for 1 hour and incubated overnight at 4 °C with the following antibodies: anti-PRDX6 (ab16947, abcam), anti-HLA-I (LS-B6775, LifeSpan Biosciences, Inc), anti-paraoxonase (PON1) (ab24261, abcam), anti-ApoA1 (home-made), or anti-catalase (ab52477, abcam). ApoA1 was detected as a loading control. Membranes were washed with TBS-T and incubated with the appropriate secondary antibody (1:2500) for 1 hour at room temperature. After 4 washes, the signal was detected with an ECL chemiluminescence kit (GE Healthcare).

Histology and immunohistochemistry. Samples of arterial wall and intra-luminal thrombus obtained from AAA patients were embedded in paraffin, and 4 µm cross-sections were cut. Ceroids were detected by direct observation of tissue by fluorescence microscopy (ceroids autofluoresce at 550 nm, producing a red signal). Immunohistochemistry was performed with antibodies against the following proteins: PRDX6 (ab16947, abcam), the lipid peroxidation marker MDA (ab6463, abcam), the neutrophil marker CD15 (Dako), and alpha smooth muscle actin (Dako). Sections were then incubated with the appropriate biotinylated secondary antibody and ABC complex, followed by staining with 3,3'-diaminobenzidine (DAB), hematoxylin counterstaining, and mounting in DPX medium.

ELISA. The plasma concentration of soluble PRDX6 in AAA and control samples was measured with a commercial ELISA kit (LF-EK0206, AbFrontier).

Statistical analysis. Data are expressed as mean ± SEM. Between-group comparisons were assessed for categorical variables with the χ^2 test and for numerical variables by Mann-Whitney non-parametric test (ELISA and western blot of controls vs patients) or ANOVA followed by Bonferroni test (western blot of *in vitro* experiment). Multivariate logistic regression analysis included only variables that were statistically significant in the univariate analysis, and was performed to assess predictors of the presence of AAA. Univariate association of PRDX6 with AAA size was assessed by the Pearson correlation test and then adjusted for age. Ninety-five percent confidence intervals (CI) were calculated for each comparison. Differences were considered statistically significant at $p < 0.05$. Statistical analysis was performed with SPSS 15.0.

References

- Jacomelli, J., Summers, L., Stevenson, A., Lees, T. & Earnshaw, J. J. Impact of the first 5 years of a national abdominal aortic aneurysm screening programme. *Br J Surg* **103**, 1125–1131, doi: 10.1002/bjs.10173 (2016).
- Salvador-González, B. *et al.* Prevalence of Abdominal Aortic Aneurysm in Men Aged 65–74 Years in a Metropolitan Area in North-East Spain. *Eur J Vasc Endovasc Surg* **52**, 75–81, doi: 10.1016/j.ejvs.2016.04.005 (2016).
- Sakalihan, N., Limet, R. & Defawe, O. D. Abdominal aortic aneurysm. *Lancet* **365**, 1577–1589, doi: 10.1016/S0140-6736(05)66459-8 (2005).
- Limet, R., Sakalihan, N. & Albert, A. Determination of the expansion rate and incidence of rupture of abdominal aortic aneurysms. *J Vasc Surg* **14**, 540–548, doi: 10.1016/0741-5214(91)90249-T (1991).
- Acosta-Martin, A. E. *et al.* Quantitative mass spectrometry analysis using PACIFIC for the identification of plasma diagnostic biomarkers for abdominal aortic aneurysm. *PLoS One* **6**, e28698, doi: 10.1371/journal.pone.0028698 (2011).
- Wallinder, J., Bergström, J. & Henriksson, A. E. Discovery of a novel circulating biomarker in patients with abdominal aortic aneurysm: a pilot study using a proteomic approach. *Clin Transl Sci* **5**, 56–59, doi: 10.1111/j.1752-8062.2011.00372.x (2012).
- Spadaccio, C. *et al.* Serum proteomics in patients with diagnosis of abdominal aortic aneurysm. *Cardiovasc Pathol* **21**, 283–290, doi: 10.1016/j.carpath.2011.09.008 (2012).
- Gamberi, T. *et al.* A proteomic approach to identify plasma proteins in patients with abdominal aortic aneurysm. *Mol Biosyst* **7**, 2855–2862, doi: 10.1039/c1mb05107e (2011).
- Burillo, E. *et al.* ApoA-I/HDL-C levels are inversely associated with abdominal aortic aneurysm progression. *Thromb Haemost* **113**, 12, doi: 10.1160/TH14-10-0874 (2015).
- Stather, P. W. *et al.* Meta-analysis and meta-regression analysis of biomarkers for abdominal aortic aneurysm. *Br J Surg* **101**, 1358–1372, doi: 10.1002/bjs.9593 (2014).
- Jorge, I. *et al.* The human HDL proteome displays high inter-individual variability and is altered dynamically in response to angioplasty-induced atheroma plaque rupture. *J Proteomics* **106**, 61–73, doi: 10.1016/j.jprot.2014.04.010 (2014).
- Vaisar, T. *et al.* Shotgun proteomics implicates protease inhibition and complement activation in the antiinflammatory properties of HDL. *J Clin Invest* **117**, 746–756, doi: 10.1172/JCI26206 (2007).
- Alwaili, K. *et al.* The HDL proteome in acute coronary syndromes shifts to an inflammatory profile. *Biochim Biophys Acta* **1821**, 405–415, doi: 10.1016/j.bbali.2011.07.013 (2012).
- Tan, Y. *et al.* Acute coronary syndrome remodels the protein cargo and functions of high-density lipoprotein subfractions. *PLoS One* **9**, e94264, doi: 10.1371/journal.pone.0094264 (2014).
- Yan, L. R. *et al.* A pro-atherogenic HDL profile in coronary heart disease patients: an iTRAQ labelling-based proteomic approach. *PLoS One* **9**, e98368, doi: 10.1371/journal.pone.0098368 (2014).
- Annama, W. & von Eckardstein, A. High-density lipoproteins. Multifunctional but vulnerable protectors from atherosclerosis. *Circ J* **77**, 2432–2448 doi: 10.1253/circj.CJ-13-1025 (2013).
- Vickers, K. C. & Remaley, A. T. HDL and cholesterol: life after the divorce? *J Lipid Res* **55**, 4–12, doi: 10.1194/jlr.R035964 (2014).
- Ortiz-Muñoz, G. *et al.* HDL antielastase activity prevents smooth muscle cell anoikis, a potential new antiatherogenic property. *FASEB J* **23**, 3129–3139, doi: 10.1096/fj.08-127928 (2009).
- Delbosc, S. *et al.* Impaired high-density lipoprotein anti-oxidant capacity in human abdominal aortic aneurysm. *Cardiovasc Res* **100**, 307–315, doi: 10.1093/cvr/cvt194 (2013).
- García-Marqués, F. *et al.* A novel systems-biology algorithm for the analysis of coordinated protein responses using quantitative proteomics. *Mol Cell Proteomics* **15**, 1740–1760, doi: 10.1074/mcp.M115.055905 (2016).
- Rosenson, R. S. *et al.* HDL Measures, Particle Heterogeneity, Proposed Nomenclature, and Relation to Atherosclerotic Cardiovascular Events. *Clin Chem* **57**, 392–410, doi: 10.1373/clinchem.2010.155333 (2011).
- McMahon, M. *et al.* Proinflammatory high-density lipoprotein as a biomarker for atherosclerosis in patients with systemic lupus erythematosus and rheumatoid arthritis. *Arthritis Rheum* **54**, 2541–2549, doi: 10.1002/art.21976 (2006).
- Han, C. Y. *et al.* Serum amyloid A impairs the antiinflammatory properties of HDL. *J Clin Invest* **126**, 796, doi: 10.1172/JCI86401 (2016).

24. Webb, N. R. *et al.* Deficiency of Endogenous Acute-Phase Serum Amyloid A Protects apoE^{-/-} Mice From Angiotensin II-Induced Abdominal Aortic Aneurysm Formation. *Arterioscler Thromb Vasc Biol* **35**, 1156–1165, doi: 10.1161/ATVBAHA.114.304776 (2015).
25. Martinez-Pinna, R. *et al.* Proteomic analysis of intraluminal thrombus highlights complement activation in human abdominal aortic aneurysms. *Arterioscler Thromb Vasc Biol* **33**, 2013–2020, doi: 10.1161/ATVBAHA.112.301191 (2013).
26. Norata, G. D., Pirillo, A., Ammirati, E. & Catapano, A. L. Emerging role of high density lipoproteins as a player in the immune system. *Atherosclerosis* **220**, 11–21, doi: 10.1016/j.atherosclerosis.2011.06.045 (2012).
27. Shiflett, A. M., Bishop, J. R., Pahwa, A. & Hajduk, S. L. Human high density lipoproteins are platforms for the assembly of multi-component innate immune complexes. *J Biol Chem* **280**, 32578–32585, doi: 10.1074/jbc.M503510200 (2005).
28. Wang, S. H., Yuan, S. G., Peng, D. Q. & Zhao, S. P. HDL and ApoA-I inhibit antigen presentation-mediated T cell activation by disrupting lipid rafts in antigen presenting cells. *Atherosclerosis* **225**, 105–114, doi: 10.1016/j.atherosclerosis.2012.07.029 (2012).
29. Soran, H., Schofield, J. D., Liu, Y. & Durrington, P. N. How HDL protects LDL against atherogenic modification: paraoxonase 1 and other dramatis personae. *Curr Opin Lipidol* **26**, 247–256, doi: 10.1097/MOL.000000000000194 (2015).
30. Burillo, E. *et al.* Paraoxonase-1 overexpression prevents experimental abdominal aortic aneurysm progression. *Clin Sci (Lond)* **130**, 10, doi: 10.1042/CS20160185 (2016).
31. Ambruso, D. R. Peroxiredoxin-6 and NADPH oxidase activity. *Methods Enzymol* **527**, 145–167, doi: 10.1016/B978-0-12-405882-8.00008-8 (2013).
32. Martinez-Pinna, R. *et al.* Identification of peroxiredoxin-1 as a novel biomarker of abdominal aortic aneurysm. *Arterioscler Thromb Vasc Biol* **31**, 935–943, doi: 10.1161/ATVBAHA.110.214429 (2011).
33. Martinez-Pinna, R., Gonzalez de Peredo, A., Monsarrat, B., Burlet-Schiltz, O. & Martin-Ventura, J. L. Label-free quantitative proteomic analysis of human plasma-derived microvesicles to find protein signatures of abdominal aortic aneurysms. *Proteomics Clin Appl* **8**, 620–625, doi: 10.1002/prca.201400010 (2014).
34. Lien, Y. C., Feinstein, S. I., Dodia, C. & Fisher, A. B. The roles of peroxidase and phospholipase A2 activities of peroxiredoxin 6 in protecting pulmonary microvascular endothelial cells against peroxidative stress. *Antioxid Redox Signal* **16**, 440–451, doi: 10.1089/ars.2011.3950 (2012).
35. Chatterjee, S. *et al.* Peroxiredoxin 6 phosphorylation and subsequent phospholipase A2 activity are required for agonist-mediated activation of NADPH oxidase in mouse pulmonary microvascular endothelium and alveolar macrophages. *J Biol Chem* **286**, 11696–11706, doi: 10.1074/jbc.M110.206623 (2011).
36. Kwon, J. *et al.* Peroxiredoxin 6 (Prdx6) supports NADPH oxidase1 (Nox1)-based superoxide generation and cell migration. *Free Radic Biol Med* **96**, 99–115, doi: 10.1016/j.freeradbiomed.2016.04.009 (2016).
37. Martin-Ventura, J. L. *et al.* Erythrocytes, leukocytes and platelets as a source of oxidative stress in chronic vascular diseases: detoxifying mechanisms and potential therapeutic options. *Thromb Haemost* **108**, 435–442, doi: 10.1160/TH12-04-0248 (2012).
38. Ambruso, D. R., Ellison, M. A., Thurman, G. W. & Leto, T. L. Peroxiredoxin 6 translocates to the plasma membrane during neutrophil activation and is required for optimal NADPH oxidase activity. *Biochim Biophys Acta* **1823**, 306–315, doi: 10.1016/j.bbamcr.2011.11.014 (2012).
39. Chowdhury, I. *et al.* Oxidant stress stimulates expression of the human peroxiredoxin 6 gene by a transcriptional mechanism involving an antioxidant response element. *Free Radic Biol Med* **46**, 146–153, doi: 10.1016/j.freeradbiomed.2008.09.027 (2009).
40. Lee, C. K. *et al.* Analysis of peroxiredoxin decreasing oxidative stress in hypertensive aortic smooth muscle. *Biochim Biophys Acta* **1774**, 848–855, doi: 10.1016/j.bbapap.2007.04.018 (2007).
41. Zarkovic, N., Cipak, A., Jaganjac, M., Borovic, S. & Zarkovic, K. Pathophysiological relevance of aldehydic protein modifications. *J Proteomics* **92**, 239–247, doi: 10.1016/j.jpro.2013.02.004 (2013).
42. Bonzon-Kulichenko, E. *et al.* A robust method for quantitative high-throughput analysis of proteomes by 18O labeling. *Mol Cell Proteomics* **10**, M110 003335, doi: 10.1074/mcp.M110.003335 (2011).
43. Navarro, P. *et al.* General statistical framework for quantitative proteomics by stable isotope labeling. *J Proteome Res* **13**, 1234–1247, doi: 10.1021/pr4006958 (2014).
44. Martinez-Acedo, P. *et al.* A novel strategy for global analysis of the dynamic thiol redox proteome. *Molecular & cellular proteomics: MCP* **11**, 800–813, doi: 10.1074/mcp.M111.016469 (2012).
45. Martínez-Bartolomé, S. *et al.* Properties of average score distributions of SEQUEST: the probability ratio method. *Mol Cell Proteomics* **7**, 1135–1145, doi: 10.1074/mcp.M700239-MCP200 (2008).
46. Navarro, P. & Vázquez, J. A refined method to calculate false discovery rates for peptide identification using decoy databases. *J Proteome Res* **8**, 1792–1796, doi: 10.1021/pr800362h (2009).

Acknowledgements

We thank Simon Bartlett for language and scientific editing. This study was supported by the Spanish Ministry of Economy and Competitiveness (MINECO) (SAF2016-80843-R, BIO2012-37926 and BIO2015-67580-P), Fondo de Investigaciones Sanitarias ISCIII-FEDER (PRB2) (IPT13/0001, ProteoRed, Redes RIC RD12/0042/00038 and RD12/0042/0056, Biobancos RD09/0076/00101 and CA12/00371), Centro de Investigación Biomédica en Red de Diabetes y Enfermedades Metabólicas Asociadas (CIBERDEM), and FRIAT. The CNIC is supported by the Spanish Ministry of Economy and Competitiveness (MINECO) and the Pro-CNIC Foundation, and is a Severo Ochoa Center of Excellence (MINECO award SEV-2015-0505).

Author Contributions

E.B. and I.J. performed all the experiments, prepared the figures and wrote the manuscript. D.M. and E.C. helped in the proteomic analysis and in the *in vitro* experiments. M.T.H. and I.E. designed and performed the quantification and statistical proteomic method. L.B.C., J.E., J.B.M. and O.M. contributed with scientific support. J.V. and J.L.M.V. designed and supervised the experiments, correct the manuscript and coordinated the project. All authors reviewed the manuscript.

Additional Information

Supplementary information accompanies this paper at <http://www.nature.com/srep>

Competing financial interests: The authors declare no competing financial interests.

How to cite this article: Burillo, E. *et al.* Quantitative HDL Proteomics Identifies Peroxiredoxin-6 as a Biomarker of Human Abdominal Aortic Aneurysm. *Sci. Rep.* **6**, 38477; doi: 10.1038/srep38477 (2016).

Publisher's note: Springer Nature remains neutral with regard to jurisdictional claims in published maps and institutional affiliations.



This work is licensed under a Creative Commons Attribution 4.0 International License. The images or other third party material in this article are included in the article's Creative Commons license, unless indicated otherwise in the credit line; if the material is not included under the Creative Commons license, users will need to obtain permission from the license holder to reproduce the material. To view a copy of this license, visit <http://creativecommons.org/licenses/by/4.0/>

© The Author(s) 2016